DEVELOPMENT OF LASER CLADDING PROCEDURE THROUGH EXPERIMENT AND ANALYSIS USING POWDER BLOWN DIRECTED ENERGY DEPOSITION

D. Garcia[1,2*], K. I. Watanabe[1,2], L. Marquez[1,2], E. Arrieta[1,2], R. Wicker[1,2], and F. Medina[1,2]

[1]Aerospace and Mechanical Engineering, University of Texas at El Paso,
El Paso, TX 79968, USA.
[2] W.M. Keck Center for 3D Innovation, El Paso, TX, USA.

* Corresponding author:
Email: dgarcia68@miners.utep.edu

Abstract

Directed Energy Deposition (DED) is one of the categories in Additive Manufacturing (AM) that has increased its popularity due to the technological advancements in recent years mainly with advancements in laser power, application of multi-materials, and capability to print greater dimensions. We are experimenting with a particular process in DED, cladding. For our experiment, we implemented a powdered feedstock (Inconel 718) which was assessed with distinct types of substrates in an effort to reduce the time spent on trial-and-error development of cladding parameters. We developed a procedure to determine a good clad interaction after an examination of the microstructure and interaction of single beads and a hatched area. The results demonstrate the ideal powers to be applied in the three substrates assessed with correlation to the dilution percentage where our target ranged from 10 to 30%.

Keywords: Inconel 625, Inconel 718, Directed Energy Deposition (DED), Cladding, Additive Manufacturing (AM)

Introduction

Additive manufacturing (AM) is the process of producing three-dimensional objects which commonly builds one layer at a time. This technology is aided by the application of 3D scanners or computer-aided design (CAD) which allows the system to manufacture complex geometric shapes [1]. In recent years, additive manufacturing has demonstrated rapid growth and interest among researchers due to its broad variety of materials, cost-effectiveness, and applications. Additive manufacturing can utilize a wide variety of materials, such as polymers, ceramics, metals, and composites. For these reasons, additive manufacturing has several applications in different industries, such as aerospace, transportation, medical, energy and consumer products. Furthermore, additive manufacturing can reduce lead times for wrought materials, significant cost and schedule reductions, printing components no longer built by the Original Equipment Manufacturers (OEMs), reduction of part by integration, etc [2]. Today, there are different additive manufacturing technologies, such as binder jetting, material extrusion, powder bed fusion, sheet lamination, and direct energy deposition.

Scope of the Study

In this research paper, our attention is focused on directed energy deposition. Specifically, in the cladding process between three varied materials which are: Inconel 718 as our feedstock, and Inconel 625, and Stainless-steel as the substrates. In a proper cladding process, it is critical to understand the proper interaction of the coating onto the substrate. Cladding is a directed energy deposition (DED) process in which metallic powder or wire feedstock is melted on metallic surfaces using a high-power laser to repair damaged surfaces or to enhance surface properties [3]. In this experiment our metal coating was Inconel 718, which is known for its high strength. Also, the process itself is one of the most time-consuming challenges; this involves finding the proper hatch width, powder feed rate, travel speed, deposit height, and understanding the interface and adhesion of the metal powder being applied onto the substrate. As mentioned, the purpose of cladding is to improve the properties of the material (yield strength, ultimate tensile strength, wear and corrosion resistance) to which the cladding is applied [4]. Being able to standardize the process of cladding by using powder blown directed energy deposition is significant. Some benefits that are achieved by this research not only include the optimization of the time-consuming process of adjusting the parameters, but also analyzing an acceptable and repeatable interaction and thermal characteristics. Additionally, obtaining a good interaction would lead to enhanced properties in the substrate, moreover a proper restoration when repairing a geometry. This research would lead to a reliable and even cost- effective process.

Materials and Methods

For this experiment the machine utilized was an RPM Innovations 222XR Laser Deposition System. The machine itself operates in 5-axis and utilizes Laser Deposition Technology (LDT) defined as the process in which metal powder is injected into the focused beam of a high-power laser under tightly controlled atmospheric conditions to perform laser repair, laser cladding, and laser free-form manufacturing [5]. The machine's gantry is capable of printing 2ft in the X-axis, 2ft in the Y-axis, 2ft in the Z-axis, and is equipped with a tilt table capable of 220º of absolute tilt position, and a rotate table capable of continuous, absolute positioning. The machine uses a 2-kilowatt Ytterbium fiber laser with a spot size ranging from 0.508 to 3.55 mm to melt powdered metal delivered by argon gas in a precision-controlled tool path. Oxygen levels were kept below 10 ppm to produce proper quality depositions during the experimentation process.

Powder Feedstock

Inconel 718 powder feedstock with a size distribution of 45-150µm from AP&C (Boisbriand, Canada) was used for the study. The powder was produced by the Advanced Plasma Atomization (APA™) process where plasma torches melt and atomize metal wire feedstock sourced from 100% virgin melted material [6].

Sample Identification and Documentation

A total of three experiments were studied for this research paper. The first experiment utilized Inconel 718 as the cladding material over Stainless-steel. The second and third portions of

the experiment involved Inconel 718 on machined and as-built Inconel 625 plates. The spot size utilized over the three samples was 1.778 mm with a spacing between each clad of 7.62 mm for the Stainless-steel and 5.08 mm for the Inconel 625 substrates. Also, the mass flow rate used among the three experiments was 11 g/min. The parameters followed for these experiments are included in **Table 1** and **Table 2**.

Table 1. Inconel 718 on Stainless-steel (As-built specimen parameters)

Name	Power (W)	Speed (mm/s)	Energy Dens. (J/mm)	Feed Rate (RPM)
Test 1	400	5.08	78.74	5
Test 2	600	7.58	79.18	5
Test 3	800	10.12	79.07	5
Test 4	1000	12.66	79.00	5
Test 5	1070	13.55	78.99	5
Test 6	1200	15.20	78.96	5
Test 7	1400	17.74	78.93	5
Test 8	1600	20.28	78.90	5

Table 2. Inconel 718 on Inconel 625 (As-built and Machined)

Name	Power (W)	Speed (mm/s)	Energy Dens. (J/mm)	Feed Rate (RPM)
Test 1	400	5.08	78.74	4.7
Test 2	600	7.58	79.18	4.7
Test 3	800	10.12	79.07	4.7
Test 4	1000	12.66	79.00	4.7
Test 5	1070	13.55	78.99	4.7
Test 6	1200	15.20	78.96	4.7
Test 7	1400	17.74	78.93	4.7
Test 8	1600	20.28	78.90	4.7
Hatch 1	800	10.12	79.07	4.7
Hatch 2	1000	12.66	79.00	4.7
Hatch 3	1200	15.20	78.96	4.7

Experiment Setup

Samples for metallography observation were first mechanically grinded, then polished, and etched. The grinding and polishing procedures were conducted with an ATM SAPHIR 530 semi-automatic system. For test 1; Inconel 718 on Stainless-steel, Kalling's No. 2 (see **Table 3**) is used for Inconel 718 and Carpenter's Etchant (see **Table 5**) for Stainless-steel 300 series. Test 2; machined Inconel 718 on Inconel 625 and Test 3; as-built Inconel 718 on Inconel 625, Etchant 1 (see **Table 4**) is used.

The grinding procedure started with a 320-grit coarse Si-C (Silicon carbide) grinding paper, followed by grits 600, 800, and 1200, each was spun at 200 RPM with a force of 22 N for 1 minute using water as a lubricant. The polishing procedure was conducted at a speed of 200 RPM and a force of 22 N for 1 minute, with each stage of the polishing process having a different disk for 6 μm, 3 μm, and 1 μm diamond suspension. Finally, the samples were polished for 30 seconds at 100 RPM with a force of 22 N using a TRICOTE polishing pad and a 0.05 μm Al_2O_3 (Alumina) suspension. The samples were placed in an ultrasonic bath in between each polishing stage to eliminate cross-contamination.

Kalling's No. 2 Etchant consists of 5 g of Cupric chloride, 10 ml of hydrochloric acid, and 100 ml of Ethanol [7]. For the etching procedure in this investigation, the specimens were swabbed with the etching solution for a range of 30 to 60 seconds. Carpenter's Etchant consists of 8.5 g of Ferric chloride, 2.4 g of Cupric chloride, 122 ml of Hydrochloric Acid, 6 ml of Nitric Acid, and 122 ml of Ethanol. The immersion of the sample was placed in the etchant for 5 seconds left out in air for another 5 seconds, then placed in DI water. Etchant 1 was used in electro etching consisting of 70 ml Phosphoric acid and 30 ml Deionized water at room temperature. Using 5 volts for 12s- 2mins depending on the size of the sample.

222XR RPM machine (DED) machine was used for the experiment setup for the cladding process. For test 1 the substrate utilized was a Stainless-steel plate. The plate was clamped into the bend of the machine by using two clamps holding the plate from both sides. The process took a total of 8 single bead tests replicated 3 times along the plate. Furthermore, the 2 last tests involved the cladding process of a hatch. An overlap of 33% was utilized for all the three hatches, each running at different power and speed. The same process was repeated for the machined plate.

Table 3. Kalling's No. 2

$CuCl_2$	5g
Hydrochloric acid	10 ml
Ethanol	100 ml

Table 4. Etchant 1

Phosphoric acid	70 ml
Deionized water	30 ml

Table 5. Carpenter's Etchant

$FeCl_3$	8.5 g
$CuCl_2$	2.4 g
Hydrochloric acid	122 ml
Nitric acid	6 ml
Ethanol	122 ml

Results and Discussion

Microstructure Characterization

Tests were conducted on eight different power and speed traits. ImageJ software was utilized for data analysis on the single beads and hatched areas. Ideally, our focus was on obtaining a dilution between 10 to 30% [8]. Dilution is described as the proportion of base material in the resultant weld metal, and for a single bead deposit, it is usually taken to be the ratio of the cross-sectional area of melted base material to the total cross-sectional area of the fusion zone [9]. **Figure 1** depicts the formula utilized to calculate dilution percentage.

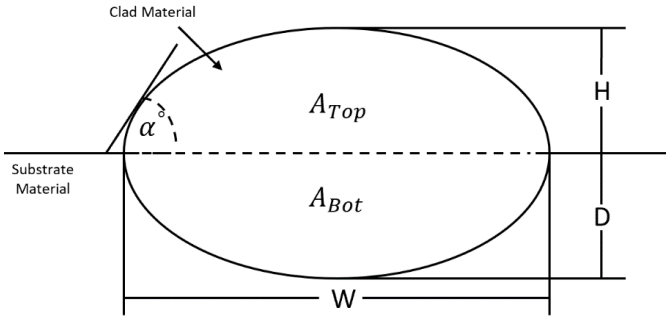

$$\text{Dilution} = \frac{\text{A}_{\text{Bottom}}}{\text{A}_{\text{Top}} + \text{A}_{\text{Bottom}}}$$

Figure 1. Dilution Formula

Test 1 - Inconel 718 on Stainless-Steel

The following single beads were obtained on the Stainless-Steel substrate. The powers used ranges from 400 W to 1600 W (see **Figure 2**).

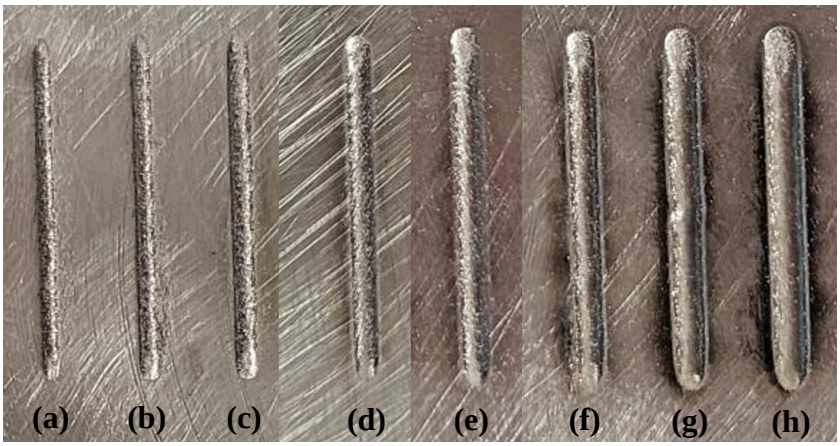

Figure 2. Single Beads on Stainless-steel: (a) 400, (b) 600, (c) 800, (d) 1000, (e) 1070, (f)1200, (g) 1400, and (h) 1600

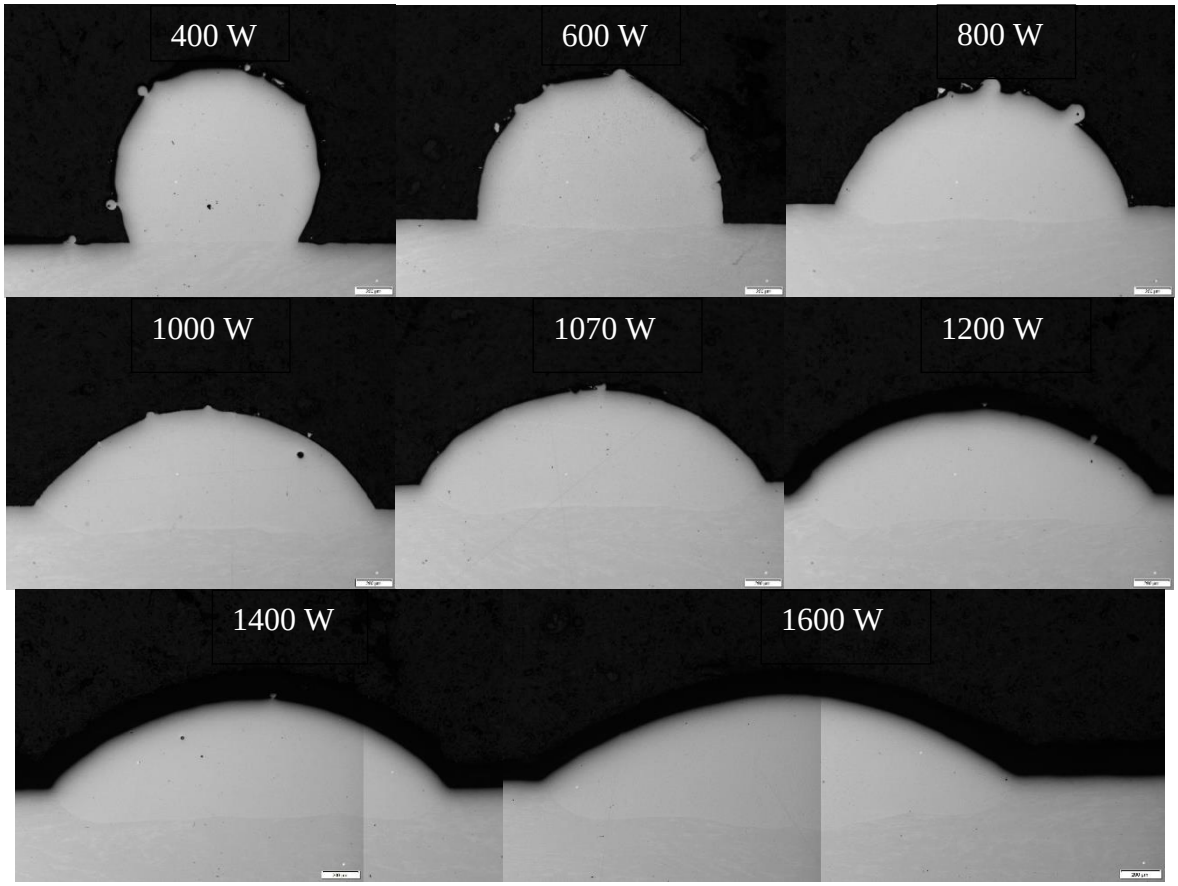

Figure 3. Microstructure of Single Beads on Stainless-steel

Figure 3 portrays the profile of the single beads done on the Stainless-steel build plate. Additionally, on **Figure 4** we were able to identify a decrease in the height of the samples as power was increased. At the same time, the width of each of the samples increased.

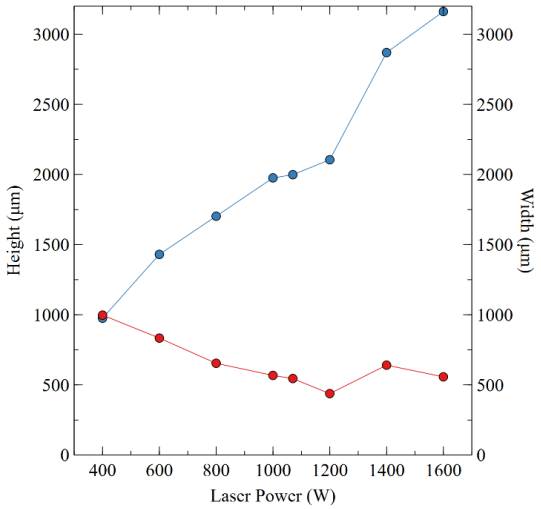

Figure 4. Height & Width vs. Power Graph on Stainless-steel

After data was obtained, a graph (see **Figure 5**) was plotted to show the interaction of dilution (red dotted line) and the contact angle (blue dotted line) in contrast to the power used in each of the samples. As mentioned before, a proper dilution is targeted to be around 10 to 30% [8]. It was concluded that the ideal candidate for a proper cladding ranged from 800 to 1200 W (see area covered by blue rectangle) for the Stainless-steel substrate.

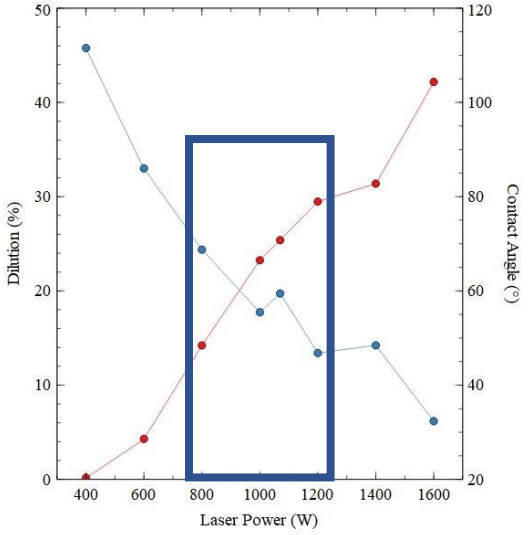

Figure 5. Dilution vs. Power Graph for Test 1

Test 2 - Machined Inconel 718 on Inconel 625

For test number two, the same process was followed. Once the data was obtained, a graph was plotted to identify the proper power range according to the dilution percentage previously defined. **Figure 6** shows the data obtained from the graph. Interesting enough, unlike Stainless-steel it was found that the ideal candidates ranged at a lower power; 600 to 800 W (see area covered by blue rectangle). Additionally, when comparing **Figure 4** and **Figure 7**, it is notable that the cladding interaction on the Inconel 625 substrate it is wider and shorter than the Stainless-steel substrate when ranging from 400 to 1200 W.

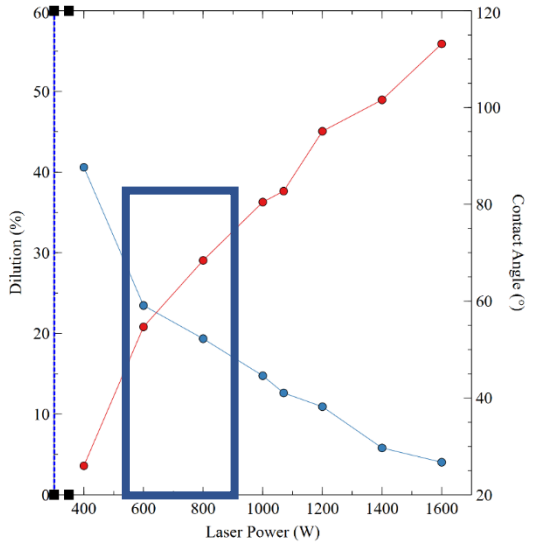

Figure 6. Dilution vs. Power Graph for Test 2

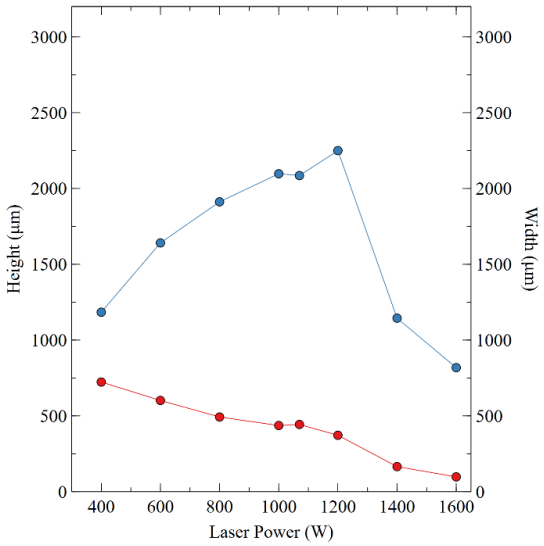

Figure 7. Height & Width vs. Power Graph on Machined Inconel 625

Test 3 – As-built Inconel 718 on Inconel 625

Unlike the machined Inconel substrate, the as-built specimen showed a lower range of power for a proper dilution. As mentioned, in **Figure 8** we can observe that the power ranged from 400 to 600 W (see area covered by blue rectangle), obtaining dilution percentages values of 16.52 to 25.46%.

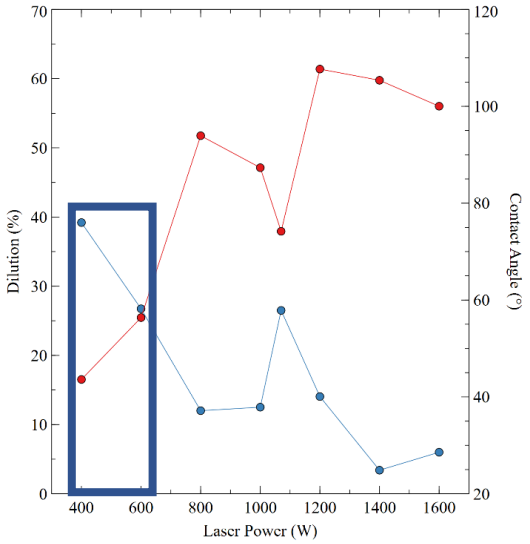

Figure 8. Dilution vs. Power Graph for Test 3

Moreover, when comparing both substrates for the Inconel 625 (machined and as-built samples) we observed a distinctive pattern in its density. **Figure 9** depicts the increase in porosity (see area covered by blue rectangle) in the as-built sample of Inconel 625. On the other hand, the machined samples presented less porosity. In essence, these results can be correlated to their manufacturing process. The additively built specimen was expected to have a lower density compared to the machined one as it didn't have any proper post-processing.

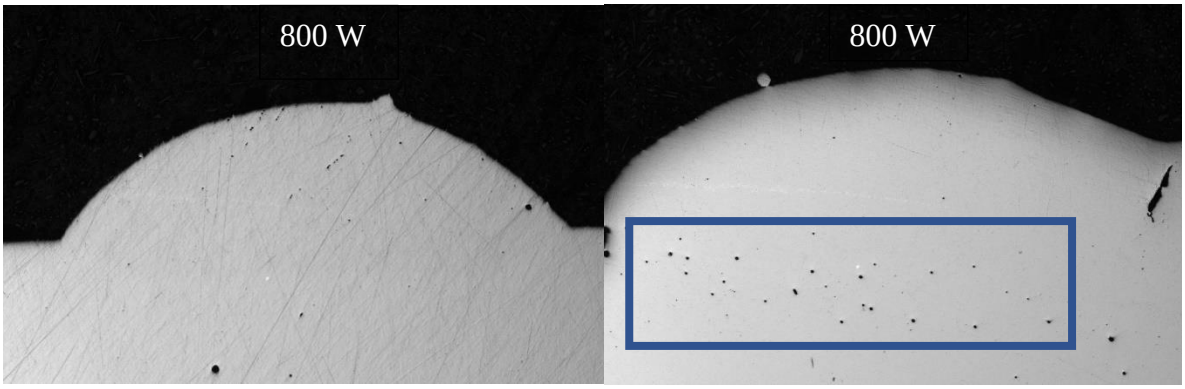

Figure 9. Comparison of Inconel Machined (Left) and As-built Samples (Right)

Conclusion

Parameters obtained both gantry speed and power) are intricately connected to chemical compatibility between the known substrate and the cladding material intended to be used. Also, a key factor commonly underestimated is surface finish. As already discussed, there was a clear quality and density improvement on the bond between the substrate and cladding material on the machined EBM Inconel 625 substrate. Parameters shown on the described research must be

analyzed and confirm that optimization of dilution does not considerably affect sample's microstructure.

Further research on the interaction of the two materials is intended to be conducted. For instance, one of the experiments that could be done is using Inconel 718 on an Inconel 625 cylinder with a vertical setup. The target of this experiment would involve building on top of the Inconel 625 bar with the purpose of assessing the interaction between the two materials by conducting a hardness test. Also, to understand the effect of the vertical building of the clads and how are the properties affected.

References

[1] What is Additive Manufacturing? definition, types and processes. TWI. (n.d.). Retrieved August 3, 2022, from https://www.twi-global.com/technical-knowledge/faqs/what-is-additive-manufacturing\

[2] Gamon, A., Arrieta, E., Gradl, P. R., Katsarelis, C., Murr, L. E., Wicker, R. B., & Medina, F. (2021, November 3). Microstructure and hardness comparison of as-built Inconel 625 alloy following various additive manufacturing processes. Results in Materials. Retrieved August 2, 2022, from https://www.sciencedirect.com/science/article/pii/S2590048X21000728

[3] Gouge, M. (2017, August 11). Conduction losses due to part fixturing during laser cladding. Thermo-Mechanical Modeling of Additive Manufacturing. Retrieved August 3, 2022, from https://www.sciencedirect.com/science/article/pii/B9780128118207000069#br0005

[4] Wolff, S. J., Gan, Z., Lin, S., Bennett, J. L., Yan, W., Hyatt, G., Ehmann, K. F., Wagner, G. J., Liu, W. K., & Cao, J. (2019, March 23). Experimentally validated predictions of thermal history and microhardness in laser-deposited Inconel 718 on Carbon Steel. Additive Manufacturing. Retrieved August 2, 2022, from https://www.sciencedirect.com/science/article/pii/S2214860418308443

[5] Navigation. Laser deposition technology: how it works - ASM International. (n.d.). Retrieved August 1, 2022, from https://www.asminternational.org/news/videos/-/journal_content/56/10192/35411335/VIDEO

[6] Powders for every technology. Advanced Powders. (n.d.). Retrieved August 2, 2022, from https://www.advancedpowders.com/powders-every-technology

[7] Voort, G. F. V. (1984). Metallography: Principles and practice. McGraw-Hill.

[8] Material-Welding. (2022, May 28). Dilution rate in welding - material welding. Material Welding - Welding and NDT Training. Retrieved August 2, 2022, from https://www.materialwelding.com/dilution-rate-in-welding/

[9] DuPont, J. N., & Marder, A. R. (n.d.). Dilution in single pass arc welds - metallurgical and materials transactions B. SpringerLink. Retrieved August 8, 2022, from https://link.springer.com/article/10.1007/BF02914913